1 # Title

2 Genomic epidemiology of syphilis reveals independent emergence of macrolide resistance
3 across multiple circulating lineages

4

5 # Authors, Affiliations

6 Mathew A. Beale[1], Michael Marks[2,3], Sharon K. Sahi[4], Lauren C. Tantalo[4], Achyuta V. Nori[5],
7 Patrick French[6], Sheila A. Lukehart[7], Christina M. Marra[4], Nicholas R. Thomson[1,8]

8 Corresponding authors: MAB, mathew.beale@sanger.ac.uk; NRT, nrt@sanger.ac.uk

9

10 [1] Parasites and Microbes, Wellcome Sanger Institute, Wellcome Genome Campus, Hinxton,
11 Cambridgeshire, UK

12 [2] Clinical Research Department, Faculty of Infectious and Tropical Diseases, London School
13 of Hygiene & Tropical Medicine, London, UK

14 [3] Hospital for Tropical Diseases, London, UK

15 [4] Department of Neurology, University of Washington, USA

16 [5] Guy's & St Thomas' NHS Foundation Trust, London, UK

17 [6] The Mortimer Market Centre CNWL, Camden Provider Services, London, UK

18 [7] Departments of Medicine and Global Health, University of Washington, USA

19 [8] Department of Pathogen Molecular Biology, Faculty of Infectious and Tropical Diseases,
20 London School of Hygiene & Tropical Medicine, London, UK

21

22 Abstract

23 Syphilis is an ancient sexually transmitted infection caused by the bacterium *Treponema*
24 *pallidum* subspecies *pallidum* and may lead to severe clinical complications. Recent years
25 have seen striking increases in syphilis diagnoses in many high income countries, with the
26 UK reporting a 148% increase in new diagnoses over 10 years. The reasons for this rise are
27 complex and multifactorial, including changing cultural, behavioural, and technological
28 factors that influence sexual networks and transmission dynamics. Previous genomic
29 analyses have suggested that one lineage of syphilis, called SS14, may have expanded
30 recently, with most syphilis caused by this lineage, and that this expansion indicates
31 emergence of a single pandemic azithromycin-resistant cluster. In this study, we used high
32 throughput sequencing of *Treponema pallidum* performed on DNA extracted directly from
33 clinical swab samples and clinically derived samples with minimal passage in the rabbit to
34 more than double the number of publicly available whole genome sequences. We used
35 phylogenomic and population genomic analyses to show that both SS14-lineage and
36 Nichols-lineage *T. pallidum* are present in contemporary patients and that SS14 is a
37 polyphyletic lineage. We further correlate the appearance of genotypic macrolide resistance
38 with multiple SS14 sub-lineages, showing that both genotypically macrolide resistant and
39 macrolide sensitive sub-lineages are spreading contemporaneously. These findings
40 demonstrate that macrolide resistance has independently evolved multiple times in *T.*
41 *pallidum*, that once evolved it becomes fixed in the genome and is transmissible, and that

these findings are not consistent with the hypothesis of SS14-lineage expansion purely due to macrolide resistance. Beyond relevance to our understanding of the current syphilis epidemic, these findings show how macrolide resistance evolves in *Treponema* subspecies. Furthermore, the evolution of macrolide resistance, despite not being first-line treatment, provides a warning on broader issues of antimicrobial resistance, and highlights the importance of stewardship and strategic planning to prevent the emergence of antimicrobial resistance.

Introduction

Syphilis is an ancient, predominantly sexually transmitted infection (STI) caused by the bacterium *Treponema pallidum* subspecies *pallidum* (TPA). If untreated, syphilis causes a multi-system disease that can progress to severe cardiovascular and neurological involvement, which can be potentially fatal. Syphilis caused a pandemic wave that swept across Renaissance Europe over 500 years ago, and remained a problem until the introduction of antibiotics in the post-World War II era[1]. Despite effective treatment with benzathine benzylpenicillin G (BPG), syphilis transmission levels fluctuated but persisted throughout the 20th century, until the AIDS crisis of the 1980s and 1990s, where changes in sexual behaviour (and possibly AIDS-related mortality), led to an overall decline in incidence in many western countries and populations[2,3].

Recent years have seen a sharp increase in syphilis cases in many high-income countries, predominantly within sexual networks of men who have sex with men (MSM)[4,5]. In the United Kingdom there was a 20% increase in reported new diagnoses between 2016 and

64 2017, and a 148% increase since 2008[6]. Similar trends have been reported in other
65 countries[4,7]. The reasons for this increase are complex and multifactorial, incorporating
66 changing behavioural patterns mediated by cultural, societal and technological changes in
67 our modern world[8], resulting in a perfect epidemiological storm. It is also possible that there
68 are bacterial changes either driving the current rise in syphilis incidence, or occurring as a
69 consequence of this increase. However, current knowledge of TPA is limited, largely because
70 the bacterium was, until recently, intransigent to *in vitro* culture[9]. Most current
71 understanding of TPA biology therefore comes from related species or from TPA cultured in
72 the *in vivo* rabbit testicular model[10]. Genomic analysis has also been limited due to low
73 levels of TPA pathogen load in patients and difficulty in readily isolating new strains.
74 Sequencing must be performed directly on clinical specimens or after passage through
75 rabbits, leading to substantial bottlenecks in genomic data generation. Recent advances
76 have enabled target enrichment of pathogen reads directly from clinical or cultured
77 specimens[11,12], and this was recently employed separately by different groups, including our
78 own, to sequence TPA and other *T. pallidum* subspecies directly from patient samples[13–15].
79
80 The availability of increasing numbers of genomic sequences enabled the first description of
81 the global TPA population structure using 31 near genome-length TPA sequences, along
82 with a small number derived from closely related species[14]. The authors described two
83 lineages within TPA; a Nichols-lineage found almost exclusively in North American
84 sequences exhibiting substantial nucleotide diversity, and a geographically widespread but
85 genetically homogeneous SS14-lineage, confirming previous analyses using multi-locus
86 sequence typing[16]. Of these two lineages, they found that 68% of tested TPA genomes

87 belonged to the SS14-lineage, and further analysis using a larger dataset of 1354 single-
88 locus molecular types (comprising 623 samples from South East Asia, 241 from the USA, 392
89 from Europe and a small number of other locations) also supported this view (94%
90 SS14-lineage).

91

92 Although penicillin resistance has never been reported in syphilis, increasing levels of
93 genotypic resistance, and clinical treatment failure, to macrolides such as azithromycin have
94 been reported[17,18], conferred by either one of two single nucleotide polymorphisms (SNPs)
95 in the 23S ribosomal sequence (A2058G and A2059G). Arora *et al* reported that 90% of
96 sequenced SS14-lineage genomes and 25% of Nichols-lineage genomes contained SNPs
97 conferring macrolide resistance; furthermore, they suggested that SS14-lineage may
98 represent a single pandemic azithromycin-resistant cluster[14].

99

100 In this study, we performed direct whole genome sequencing on 73 TPA samples from the
101 US and Europe, and combined these data with 49 publicly available genomes. We used
102 phylogenetic analysis to delineate sub-lineages within the both the SS14- and Nichols-
103 lineages, showing striking patterns of the emergence and fixation of macrolide resistance
104 SNPs that indicate independent evolution and proliferation of resistance alleles. These
105 findings have implications for our understanding of the increasing incidence of syphilis and
106 on the potential of the WHO Yaws eradication campaign to drive further development of
107 macrolide resistance in both TPA and in the closely related *Treponema pallidum* subspecies
108 *pertenue* (TPP)[19,20].

109

110 Results

111 We sequenced eight genomes directly from clinical swabs collected in 2016 from patients in
112 the United Kingdom and 60 isolate genomes from low rabbit passage samples (no more
113 than two passages from the original patient sample; henceforth referred to as 'recently
114 clinically derived') originally collected from patients between 2001-2011 in the USA. We also
115 resequenced three clonally derived laboratory strains from the USA that have been
116 previously sequenced (Nichols Houston E, Nichols Houston J, Nichols Houston O) but remain
117 unpublished, and two strains for which the sequencing reads were not publicly available
118 (Chicago[21], Seattle 81-4[22]). We combined our data with 49 high-quality genomes published
119 previously[13,14,23–28], 41 of which were recently derived from clinical patients, yielding a
120 dataset of 122 genomes (109 with limited passage from clinical patients). Combined, our
121 sample set included 72 genomes from the USA (predominantly Seattle), 8 from the UK
122 (exclusively London), 9 from China (predominantly Shanghai), 23 from Portugal (exclusively
123 Lisbon), and a small number from other countries, all collected between 1912-2016
124 (Supplementary Table 1).

125

126 After removal of recombinant and repetitive sites (both by selective mapping and screening
127 – see Methods and Supplementary Table 2), we performed phylogenomic analyses, using
128 maximum likelihood and Bayesian methods to define lineages. In agreement with previous
129 studies[14], we show the presence of two dominant lineages in our dataset (previously
130 denoted SS14 and Nichols; Figure 1) that are separated by >70 non-recombining single

131 nucleotide polymorphisms (SNPs). Of the 122 total samples included in this study, 105 (86%)
132 belonged to the SS14-lineage, whilst of the 109 clinical samples included, 103 (94%) were
133 from SS14-lineage. In contrast, only six Nichols-lineage samples were recently clinically
134 derived, and most (11/17) Nichols-lineage genomes examined were historically passaged
135 isolates, including those derived from the original Nichols strain isolated in 1912 and
136 disseminated to different North American laboratories; some Nichols-lineage genomes
137 represent clones of the parent strain derived *in vivo*. However, although we observed a
138 strong bias towards clinically derived SS14-lineage samples in this dataset, not all recent
139 clinical strains were of the SS14-lineage; six recent clinical samples belonged to the Nichols-
140 lineage, three (of eight sequenced) clinical samples from the UK in 2016, one collected in
141 the Netherlands in 2013, and two from the USA in 2004, indicating that transmission of this
142 lineage is ongoing and potentially more widespread than previously thought.

143

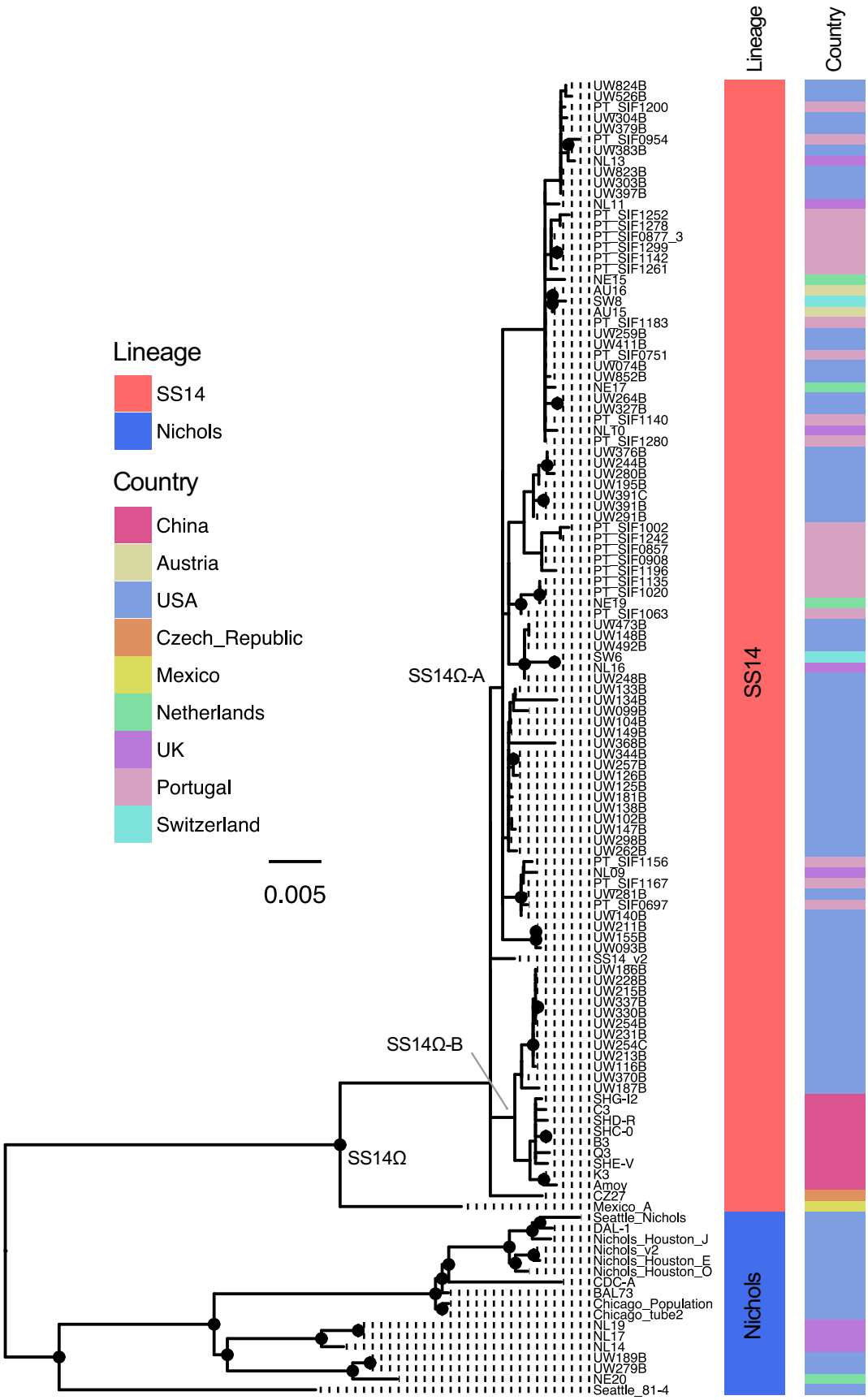
Lineage
SS14
Nichols
Country
China
Austria
USA
Czech_Republic
Mexico
Netherlands
UK
Portugal
Switzerland
0.005
SS14Ω-A
SS14Ω-B
SS14Ω
Lineage
Country
SS14
Nichols
UW824B
UW526B
PT_SIF1200
UW304B
UW379B
PT_SIF0954
UW383B
NL13
UW823B
UW303B
UW397B
NL11
PT_SIF1252
PT_SIF1278
PT_SIF0877_3
PT_SIF1299
PT_SIF1142
PT_SIF1261
NE15
AU16
SW8
AU15
PT_SIF1183
UW259B
UW411B
PT_SIF0751
UW074B
UW852B
NE17
UW264B
UW327B
PT_SIF1140
NL10
PT_SIF1280
UW376B
UW244B
UW280B
UW195B
UW391C
UW391B
UW291B
PT_SIF1002
PT_SIF1242
PT_SIF0857
PT_SIF0908
PT_SIF1196
PT_SIF1135
PT_SIF1020
NE19
PT_SIF1063
UW473B
UW148B
UW492B
SW6
NL16
UW248B
UW133B
UW134B
UW099B
UW104B
UW149B
UW368B
UW344B
UW257B
UW126B
UW125B
UW181B
UW138B
UW102B
UW147B
UW298B
UW262B
PT_SIF1156
NL09
PT_SIF1167
UW281B
PT_SIF0697
UW140B
UW211B
UW155B
UW093B
SS14_v2
UW186B
UW228B
UW215B
UW337B
UW330B
UW254B
UW231B
UW254C
UW213B
UW116B
UW370B
UW187B
SHG-I2
C3
SHD-R
SHC-0
B3
Q3
SHE-V
K3
Amoy
CZ27
Mexico_A
Seattle_Nichols
DAL-1
Nichols_Houston_J
Nichols_v2
Nichols_Houston_E
Nichols_Houston_O
CDC-A
BAL73
Chicago_Population
Chicago_tube2
NL19
NL17
NL14
UW189B
UW279B
NE20
Seattle_81-4

145 Figure 1. Maximum likelihood phylogeny of 122 high quality *T. pallidum* subspecies *pallidum*

146 genomes (including clinical and non-clinically derived samples), showing lineage and country

147 of origin. Ultra-Fast bootstrap values >=95% are labelled with black nodes points. Branches

148 are scaled by mean nucleotide substitutions/site.

149

150 Bayesian phylogenetic reconstruction was used to date the time to most recent common
151 ancestor (TMRCA) for the different TPA lineages. However, temporal analysis of heavily
152 passaged laboratory strains (such as those derived from the original Nichols isolate) is
153 problematic because the true mutational age may be unknown, meaning coalescent date is
154 difficult to infer; we therefore removed extensively passaged strains or strains with no
155 record of their passage history from this particular part of the analysis. This included the
156 removal of the Nichols and SS14 reference strains, as well as the Mexico A strain that
157 delineated the SS14Ω lineage described previously[14]. Root-to-tip regression analysis of the
158 remaining 109 clinical genomes indicated that TPA possesses a clock-like signal
159 (Supplementary Figure 1), and we performed Bayesian phylogenetic reconstruction and tip
160 date analysis using BEAST[29] under a Strict Constant model, inferring a median molecular
161 clock rate of 2.28×10^{-7}, or 0.26 sites/genome/year (meaning we would expect TPA genomes
162 on average to accumulate one SNP every four years by natural drift). We inferred a
163 temporal timeline for the tree, and our analysis broadly supported previous estimates[14]
164 dating the separation of Nichols- and SS14 at around the mid 18th Century (median date
165 1755, 95% HPD 1651–1835; Figure 2A).

166 <u>SS14-lineage shows a polyphyletic structure</u>

167 Within the SS14-lineage, the high number of full-length sequences enabled fine-scale
168 description of phylogenetic sub-structure. In particular, we show partitioning of the SS14Ω
169 centroid cluster previously defined[14] into two lineages; one composed of European and
170 North American derived samples (SS14Ω-A), and another of Chinese and North American
171 derived samples (SS14Ω-B) (Figure 1). While the American and European samples belonging
172 to the former SS14Ω-A lineage are geospatially admixed, those of the latter SS14Ω-B lineage

173 can be further separated between Chinese and North American samples. These partitions
174 were well supported in our maximum likelihood (Figure 1) and Bayesian phylogenies (Figure
175 2A), as indicated by black node points. We used the rPinecone package[30] to formally classify
176 these sub-lineages based on a defined root-to-tip SNP distance, identifying eight sub-
177 lineages (one of which we further subdivided into sublineages 1A and 1B to aid analysis
178 based temporal and geospatial divergence) within SS14-lineage that correlated well with the
179 population structure described by the phylogeny (Figure 2A). Importantly, while some nodes
180 close to the tips in our phylogeny are unsupported due to small numbers of differentiating
181 SNPs, all sub-lineages defined by rPinecone are supported by >91% posterior support at the
182 key nodes in our Bayesian phylogeny (Figure 2A).

183

184

185

186

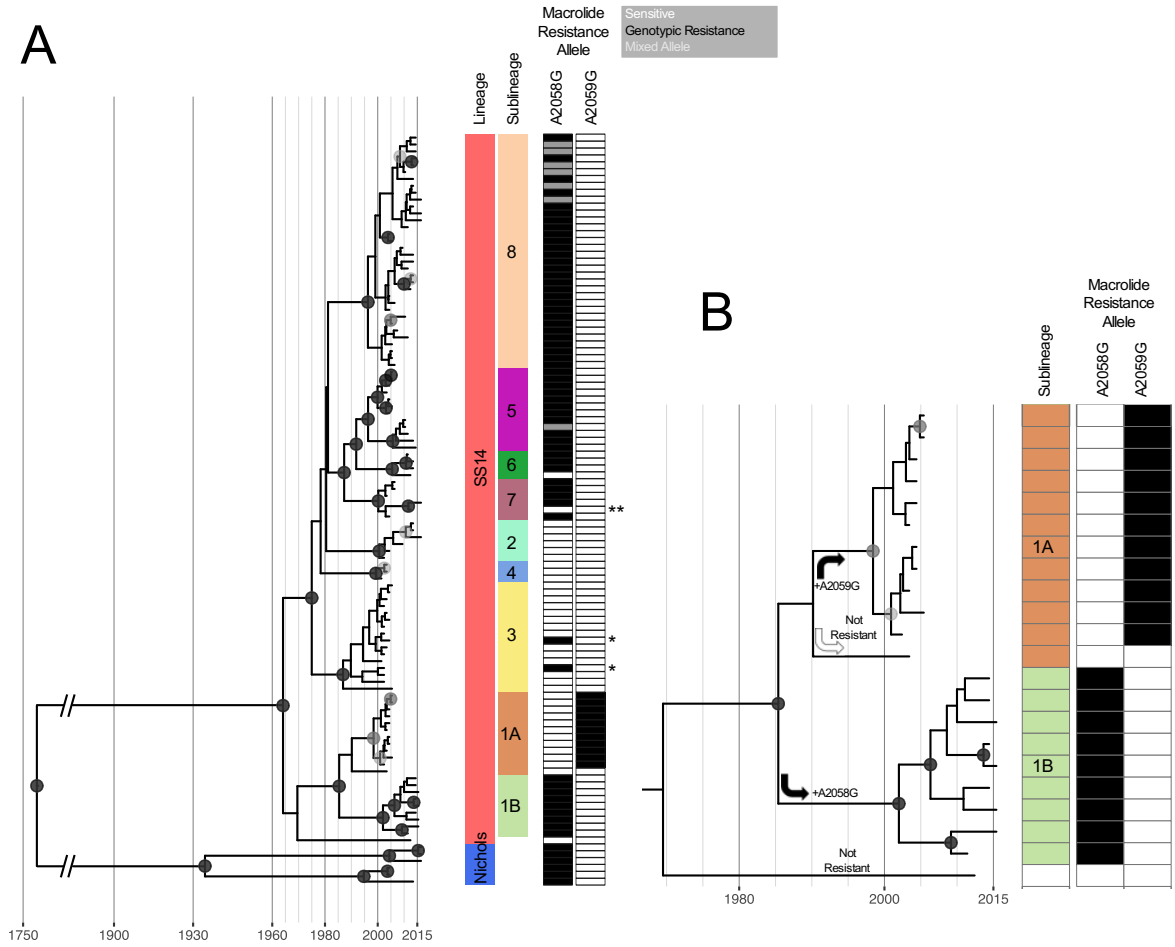

187

188 Figure 2. Bayesian maximum credibility phylogeny of sequences recently derived from

189 clinical samples shows expansion of discrete sub-lineages within SS14-lineage, with

190 independent evolution of macrolide resistance. A – Time-scaled phylogeny of all clinical

191 genomes. Coloured tracks indicate lineage, sub-lineage, and presence of macrolide

192 resistance conferring 23S rRNA SNPs (black=present, white=absent, grey=mixed). Node

193 points are shaded according to posterior support (black ≥96%, dark grey >91%, light grey

194 >80%). *Sporadic (non-lineage associated) gain of resistance is highlighted in sub-lineage 3

195 (samples UW133B and UW262B). **Possible reversion from resistant to wildtype (sample

196 SW6). B – Expanded view of sub-lineages, showing independent acquisition and fixation of

197 macrolide resistance alleles.

198

199 Macrolide resistance has evolved independently within SS14

200 The molecular basis for macrolide resistance has been well documented in *T. pallidum*, and
201 is mediated by point mutations in the 23S ribosomal RNA gene at nucleotide positions 2058
202 and 2059[31–33]. The A2058G variant was first identified in *T. pallidum* Street Strain-14 (the
203 prototype sample for the SS14-lineage), isolated as long ago as 1977[31], yet resistance has
204 not previously been analysed in context with a detailed whole genome phylogeny. We used
205 ARIBA[34] to perform localised assembly and variant calling of treponema-specific 23S
206 ribosomal sequences from all genomes, and these data were used to infer the presence of
207 both A2058G and A2059G 23S variants that confer macrolide resistance[31]. *T. pallidum*
208 possesses two copies of the 23S ribosomal RNA gene, yet previous analyses have not
209 identified heterozygosity between these two copies – where resistance alleles have been
210 sequenced, they are homozygous between 23S copies, and it has been suggested a gene
211 conversion unification mechanism may exist to facilitate this[18]. Of the 122 genomes, 83
212 showed evidence of genotypic resistance to macrolides, with 76 genomes showing >95%
213 read support for either the A2058G or A2059G variant. Since it is not possible to
214 discriminate between short reads originating from either copy of 23S because they are
215 perfect repeats, this suggests that both copies carry the same resistance mutation. Seven
216 clinically derived genomes (one UK sample from this study, six described by Pinto and
217 colleagues[13]) showed a mixed 23S allelic profile. All of these samples had >179x read
218 coverage for those sites, with only a fraction of reads (26% - 94%) possessing a resistance
219 allele. In these cases it was not possible to clearly distinguish between a mixture of
220 homozygous positive and negative bacteria in the same patient (either due to within-host
221 evolution or coinfection with multiple strains) or heterozygous sequences from a single
222 bacteria (different 23S rRNA alleles at each copy; heterozygosity in phase) (Figure 2A).

223

224 Within the 122 genomes included in this study, we observed that 67% (70/105) of SS14-
225 lineage samples and 35% (6/17) of Nichols-lineage samples were homozygous for either
226 A2058G or the A2059G 23S rRNA allele. In the SS14-lineage, samples possessed either the
227 A2058G (n=59) or the A2059G (n=11) variant. In the Nichols-lineage, six possessed a
228 resistance allele, of which all showed the A2058G variant, and all were from recent clinically
229 derived samples.

230

231 To explore the emergence of macrolide resistance, we correlated the taxa in our time-scaled
232 phylogeny with the presence of resistance alleles (Figure 2A). We observed a strong
233 correlation between our well supported sub-lineages and genotypic macrolide resistance or
234 sensitivity, such that resistance appears to have evolved on multiple occasions in a stepwise
235 manner (Figure 2A). For example, Figure 2B shows how the wildtype ancestor of sub-lineage
236 1B sequences evolved the A2058G between the late 1980s and late 1990s, contrasting with
237 sub-lineage 1A sequences which did not gain A2058G, but subsequently and independently
238 evolved the A2059G variant.

239

240 More broadly in the phylogeny, we observe that similar independent 23S rRNA mutations
241 have occurred on at least four occasions (Figure 2A), with separate sub-lineages
242 characterised by either predominantly macrolide resistant or sensitive genotypes; six of the
243 nine sub-lineages were predominantly resistant to macrolides, with three sub-lineages
244 being predominantly sensitive. Several of the macrolide sensitive sub-lineages (in particular

245 sub-lineage 3) contained similar numbers of samples as many of the resistant sub-lineages

246 (Figure 3), suggesting ongoing selection for macrolide resistance has not influenced the

247 expansion of these sub-lineages.

248

249 To examine sub-lineage expansion in greater detail, we extracted sampling dates according

250 to sub-lineage, and correlated these data with the predicted time to most recent common

251 ancestor (TMRCA) (Figure 3). Whilst all clinical sequences included in this analysis were

252 sampled after 2000, our analysis indicates that the origins of most of the sub-lineages

253 predated this time and likely arose during the 1990s (Figure 3). Regarding whole sub-lineage

254 associated resistance, we also observed more recent sporadic appearance of resistance

255 mutations, with two separate A2058G variants detected in sub-lineage 3 (an otherwise

256 macrolide sensitive sub-lineage)(Fig. 2).

257

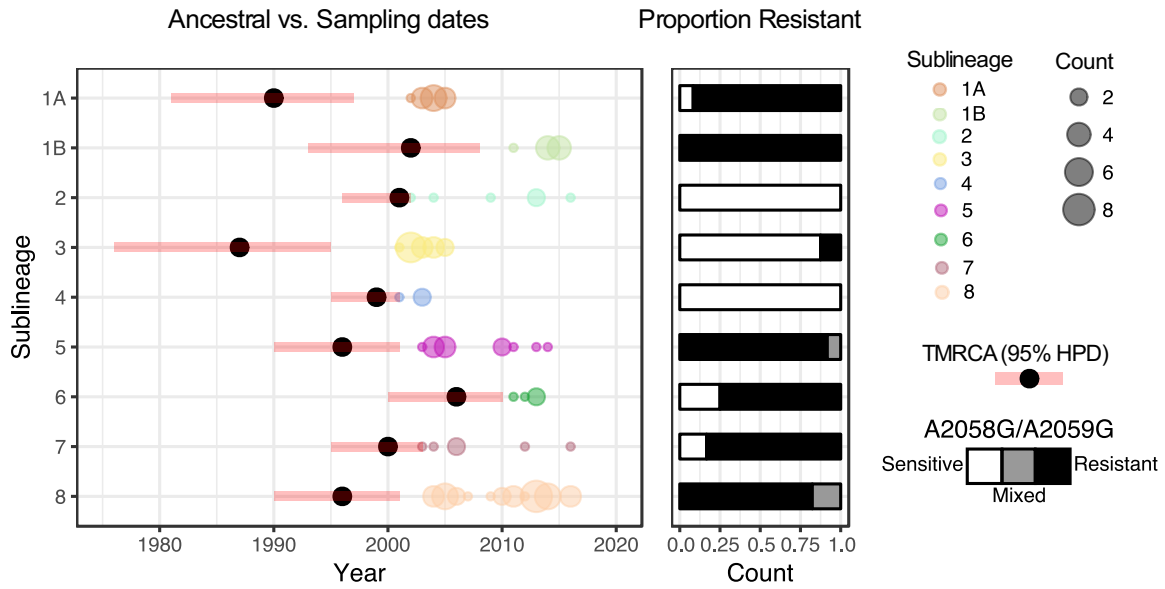

258

259 Figure 3. Macrolide resistant and sensitive SS14 sub-lineages evolved independently prior to
260 2006 and expanded equally regardless of resistance genotype. Figure 3 shows sample
261 collection dates grouped by sub-lineage, with size of circle proportional to number of
262 sequences, and showing predicted time to most recent common ancestor (TMRCA) with
263 95% highest posterior density (HPD), and proportion of genotypically macrolide resistant,
264 sensitive and mixed samples.

265 ## Discussion

266 Compiling the largest *Treponema pallidum* subspecies *pallidum* sequence collection to date,
267 we show that the majority of the contemporary samples sequenced here were from the
268 SS14-lineage, consistent with other reports[14]. However, three of eight UK genomes (38%)
269 belonged to the Nichols-lineage, showing that these two lineages are still circulating
270 concurrently, and that the prevalence of Nichols-lineage strains may vary by sampling
271 population.

272

273 We were able to reconstruct a time-scaled phylogeny using only recently clinically derived
274 samples, and the increase in whole genome sequence numbers combined with the removal
275 of heavily passaged samples contrasts with previous approaches[14,23]. Arora *et al*. reported a
276 mean evolutionary rate of 6.6 $\times 10^{-7}$ substitutions/site/year for *T. pallidum*[14], comparable
277 with free-living bacterial pathogens with environmental life cycles such as *Vibrio cholerae*
278 (6.1 $\times 10^{-7}$)[35] and *Shigella sonnei* (6.0 $\times 10^{-7}$). However, *T. pallidum* is a host-restricted
279 pathogen with substantial periods of latency, and as such we would expect a molecular
280 clock rate more similar to that of *Chlamydia trachomatis* (2.15 $\times 10^{-7}$)[36]. Our inferred rate for
281 TPA (2.28 $\times 10^{-7}$) is consistent with this expectation, as well as with other observations that
282 suggest *T. pallidum* has a low evolutionary rate[37].

283

284 Within the SS14-lineage, we defined nine well supported sub-lineages that all diverged from
285 their most recent common ancestors prior to 2006, with the earliest (sub-lineage 3)
286 potentially emerging at the end of the 1980s. We observed clear associations between

287 these nine sub-lineages and the presence of macrolide resistance conferring SNPs, with
288 each sub-lineage dominated by either macrolide resistant (n=6) or macrolide sensitive (n=3)
289 samples; there were no sub-lineages representing an even mix of resistance genotypes.
290 Such observations are not consistent with the hypothesis of an ancestrally resistant SS14-
291 lineage driven to high frequency in the population due to a fitness advantage conferred by
292 macrolide resistance, where we would expect to see expansion of a single resistant lineage.
293 Rather, we see evidence of multiple sub-lineages independently evolving macrolide
294 resistance alleles, as a likely consequence of intermittent selective pressure from macrolide
295 treatment, consistent with molecular typing data from Seattle[38]. Phylogenetic
296 reconstruction shows *de novo* evolution of macrolide resistance in syphilis is not a rare
297 event, and furthermore, when resistance evolves in a lineage, it persists in descendants,
298 resulting in transmission from person to person. That the variants appear stable within
299 lineages, with only a single instance in the phylogeny that might represent reversion to a
300 wildtype state, suggests that there is no strong fitness cost associated with possessing these
301 macrolide resistance mutations.

302

303 Although our data strongly suggest that global expansion of the SS14-lineage is not
304 contingent on macrolide resistance, the global increases seen in macrolide resistant
305 syphilis[18], as well as the number of resistant lineages emerging in our data, are a cause for
306 concern. Macrolides such as azithromycin are not considered frontline treatment for
307 syphilis, with WHO and US guidelines recommending treatment with BPG[39,40], with
308 doxycycline recommended as a secondary treatment option. In contrast, WHO now
309 recommends azithromycin rather than BPG as the treatment of choice for mass drug

310 administration and the eradication of yaws[19], caused by the closely related *T. pallidum*
311 subspecies *pertenue*. Macrolide resistance has recently been described in yaws[20] and our
312 data suggest that further independent evolution of azithromycin resistance is highly likely,
313 which would have significant implications for yaws eradication efforts. Worryingly, applying
314 azithromycin-based mass drug administration to populations infected with both TPP and
315 TPA could promote resistance in both species.

316

317 Several factors are likely to have driven the repeated evolution and subsequent expansion
318 of macrolide resistant lineages of TPA. Use of azithromycin, or other macrolides, for other
319 indications is likely to have played a significant role[41]. Azithromycin entered global markets
320 between 1988 and 1991 (marketed by Pfizer as Zithromax), and became one of the most
321 widely used antibiotics in the United States for a wide variety of indications[42], including the
322 treatment of respiratory tract infections and for the treatment of other sexually transmitted
323 infections. In many cases, the dose used for treatment of these indications is lower than the
324 recommended dose for the treatment of syphilis. Azithromycin and clarithromycin were
325 also widely used prophylactically amongst individuals living with HIV prior to the widespread
326 availability of combined anti-retroviral therapy. Off-target macrolide exposure is of
327 particular concern because azithromycin has a long half-life[43] and may persist at subclinical
328 concentrations in patients. Widespread use of macrolides for this broad range of indications
329 might therefore have contributed to sub-therapeutic exposure of patients with incubating
330 or early syphilis and ultimately selection of resistance.

331

332 The recent increase in incidence of syphilis in high income countries likely reflects changes
333 in sexual behaviour[8]. The fact that we observe the expansion of both genotypically resistant
334 and sensitive lineages highlights particular treatment issues. There have been significant
335 global shortages of BPG[44] in low, middle, and high income nations, including the United
336 States, with the global supply of BPG dependent on just three manufacturers of the active
337 ingredient[44]. Pharmaceutical production of sterile, injectable β-lactam derived
338 antimicrobials such as BPG is costly, yet as an older off-patent medication with declining
339 demand in the face of growing antimicrobial resistance (AMR) in other organisms, the
340 financial rewards for production are low[44]. This may be compounded by a misperception
341 that BPG is an outdated drug that could be replaced by newer, more effective drugs[44]. In
342 circumstances where azithromycin is used instead of doxycycline as second line treatment, a
343 shortage of BPG leads inevitably to inadequate treatment of early infectious syphilis and
344 contributes to ongoing, unchecked transmission. In China for example, studies have
345 reported that despite high rates of macrolide resistance,[45] clinicians have inappropriately
346 been resorting to macrolide treatment due to ongoing BPG shortages[46]. Thus although a
347 well-established, highly effective treatment for syphilis (BPG) has been available since the
348 mid-1950s, shortages in the present era contribute to suboptimal treatment strategies and
349 continued use of drugs with a known resistance problem.

350

351 The epidemic of syphilis and the widespread problems of azithromycin resistance and BPG
352 shortage require a multi-faceted response. This includes new strategies for treatment and
353 reduction of transmission, finding ways to improve the security of the BPG supply chain, and
354 strengthening molecular surveillance for antimicrobial resistance in *T. pallidum*[47]. Many

355 authors have discussed the importance of rethinking the economics of antimicrobial
356 development pipelines to ensure we are still able to treat infections[48,49]. In syphilis, we must
357 rethink how we can protect the continued production of existing highly efficacious
358 penicillins in the face of increasing antimicrobial resistance rendering them ineffective for
359 other organisms, especially in the light of the recent increases in syphilis incidence in
360 Europe, North America, and Asia.

361

362 Materials and Methods

363 Samples

364 UK samples consisted of residual DNA, extracted from clinical swabs using a QIAsymphony
365 (Qiagen) from routine diagnostic samples obtained from patients presenting with clinical
366 evidence of syphilis at the Mortimer Market Centre, London. Use of the UK samples was
367 approved by the NHS Research Ethics Committee (IRAS Project ID 195816). US samples
368 from Seattle were collected from individuals enrolled in a study of cerebrospinal fluid
369 abnormalities in patients with syphilis, with ethical approval at the University of Washington
370 (UW IRB # STUDY00003216). Specifically, 2.4-3.0 ml participant blood was inoculated into
371 rabbit testes as previously described[50], and *T. pallidum* suspensions were collected after the
372 second round of passage. Historical strains were propagated in rabbits and harvested from
373 infected testes. *T. pallidum* suspensions were treated using a lysis buffer (10mM Tris pH 8.0,
374 0.1M EDTA pH 8.0, 0.5% SDS), freeze-thaw, and extraction using QIAamp Mini kit (Qiagen)
375 according to the manufacturer's instructions; in select cases the proteinase K incubation
376 was extended overnight to improve DNA yield. Treponemal DNA was quantified using a

377 qPCR targeting the Tp0574 gene that is conserved across all known members of the
378 *T. pallidum* cluster, and compared to a standard curve derived from a plasmid containing
379 the PCR amplicon. Samples with a concentration >2000 genome copies/μl were selected for
380 sequencing; borderline samples with high volume and a pathogen load over 500 genome
381 copies/μl were concentrated using a vacuum centrifuge. Samples were arranged in groups
382 of 20 according to similar (within 2 C_T) treponemal load, with high concentration outlier
383 samples diluted as necessary. We added 4μl pooled commercial human gDNA (Promega) to
384 all samples to ensure total gDNA > 1μg/35μl, sufficient for library prep.

385 Sequencing

386 Genomic DNA was sheared to 100-400bp by ultrasonication, followed by adaptor ligation
387 and index barcoding according to existing Illumina protocols. Samples were pooled in the
388 preassigned groups of 20 to generate equimolar Total DNA pools. Each pool was then
389 hybridised using SureSelect 120-mer RNA baits designed against published RefSeq examples
390 of *T. pallidum* and *T. paraluiscuniculi* as described previously[15]. Libraries were subjected to
391 125bp paired end sequencing on Illumina HiSeq 2500 with version 4 chemistry according to
392 established protocols. Raw sequencing reads were deposited at the European Nucleotide
393 Archive (ENA) under project PRJEB20795; all accessions used in this project are listed in
394 Supplementary Table 1.

395 Sequence analysis and phylogenetics

396 Treponemal sequencing reads were prefiltered using a Kraken[51] v0.10.6 database containing
397 all bacterial and archaeal nucleotide sequences in RefSeq, plus mouse and human, to
398 identify and extract those reads with homology to Treponema species, followed by adaptor
399 trimming using Trimmomatic[52] v0.33. To reduce bias due to variable read depth, as well as

400 make analysis computationally tractable, for samples with high read counts we used seqtk
401 v1.0 (available at https://github.com/lh3/seqtk) to randomly down-sample the binned and
402 trimmed reads to 2,500,000 unique treponemal read pairs. For publicly available genomes,
403 raw sequencing reads were downloaded from SRA and subjected to the same binning and
404 down-sampling pipeline. For a small minority of public genomes, raw sequencing reads were
405 not available; for these we simulated 125bp PE perfect reads from the RefSeq closed
406 genomes using Fastaq (available at https://github.com/sanger-pathogens/Fastaq).

407

408 For phylogenetic analysis, we used a reference mapping approach with a custom version of
409 the SS14 v2 reference sequence (NC_021508.1) from which we first masked 14 highly
410 repetitive or recombinogenic genes (12 repetitive Tpr genes A-L, arp and TPANIC_0470)
411 using bedtools[53] v2.17.0 'maskfasta'. We mapped prefiltered sequencing reads to the
412 reference using BWA mem[54] v0.7.17 (MapQ ≥ 20), followed by indel realignment using
413 GATK[55] v3.4-46 IndelRealigner, deduplication with Picard MarkDuplicates v1.127 (available
414 at http://broadinstitute.github.io/picard/), and variant calling and consensus
415 pseudosequence generation using using samtools v1.2[56] and bcftools v1.2, requiring a
416 minimum of three supporting reads per strand and eight in total to call a variant, and a
417 variant frequency/mapping quality cut-off of 0.8; sites not meeting these criteria were
418 masked to 'N' in the pseudosequence. Importantly, reads mapping to multiple genomic
419 positions were marked and excluded from SNP calling, meaning repeated regions such as
420 the duplicated 23S genes was not included in the multiple sequence alignment used to
421 derive the phylogenies.

422

423 Multiple sequence alignments were screened for evidence of recombination using
424 Gubbins[57], generating recombination-masked full genome length and SNP-only alignments.
425 Maximum likelihood phylogenies were calculated on SNP-only alignments using IQ-Tree
426 v1.6.3[58], correcting for missing constant sites using the built in ascertainment bias
427 correction[59], allowing the built-in model testing[60] to determine a K3P (three substitution
428 types model and equal base frequencies) substitution model[61] with a FreeRate model of
429 heterogeneity[62] assuming three categories, and performing 1000 UltraFast Bootstraps[63,64].

430

431 To determine SS14 sub-lineages, we recalculated a maximum likelihood tree as described
432 above for SS14-clade sequences only (using the Mexico A strain, NC_018722.1 as outgroup),
433 before performing a joint ancestral reconstruction[65] of SNPs on the tree branches using
434 pyjar (available at https://github.com/simonrharris/pyjar). We then used the rPinecone
435 package[64] (available at https://github.com/alexwailan/rpinecone), which applies a root-to-
436 tip approach to defining clusters based on SNP distance relative to ancestral nodes. We used
437 a cluster threshold of 10 SNPs, which proved optimal for describing the underlying
438 phylogenetic structure of the tree, and yielded eight sub-lineages. Within sub-lineage 1, we
439 found that pinecone clusters did not accurately represent the phylogeny, despite a clear
440 phylogenetic separation, with one group of sequences from China associated with the
441 A2058G allele, and the other group from the USA associated with the A2059G allele. We
442 further manually clustered these sequences according to their shared ancestral nodes,
443 naming them sublineages 1A and 1B.

444

445 We evaluated our maximum likelihood phylogeny for evidence of temporal signal using
446 TempEst[66] v1.5, and this showed a correlation of 0.44 and R^2 of 0.20 for the whole tree
447 (Supplementary Figure 1), whilst the SS14-lineage -only alignment showed a correlation of
448 0.66 and R^2 of 0.44; this indicated that there was sufficient evidence for temporal signal and
449 we proceeded to BEAST analysis. BEAST[29] v1.8.2 was initially run on a recombination-
450 masked SNP-only alignment containing 284 variable sites, applying a correction for invariant
451 sites using the constantPatterns argument, in triplicate using an Uncorrelated Relaxed Clock
452 model, assuming constant population size, lognormal population distribution, GTR
453 substitution model, diffuse gamma distribution prior (shape 0.001, scale 1000), with a
454 burnin of 10 million cycles followed by 100 million MCMC cycles. All MCMC chains
455 converged, and on inspection of the marginal distribution of ucld.stdev we could not reject
456 a Strict Clock. We therefore repeated the analysis using a Strict Clock model, using the same
457 models and priors and assuming a starting molecular clock rate of 3.6×10^{-4} as described by
458 others[14]. We used the Marginal Likelihood Estimates from the triplicate BEAST runs as input
459 to Path Sampling and Stepping Stone Sampling analyses[67,68] and determined that the Strict
460 Constant model was optimal for this dataset. To further confirm the temporal signal in our
461 tree, we used the TIPDATINGBEAST package[69] in R[70] to resample tip-dates from our
462 alignment, generating 20 new datasets with randomly assigned dates – BEAST analysis using
463 the same Strict Clock prior conditions found no evidence of temporal signal in these
464 replicates, indicating that the signal in our tree was not found by chance (Supplementary
465 Figure 2).

466

467 Macrolide resistant SNPs were inferred using ARIBA[34], which performs localised assembly
468 and mapping in comparison with a custom reference database containing 23S sequences
469 from Nichols (NR_076156.1) and SS14 reference strains (NR_076531.1).

470

471 Processing of data, and all statistical analysis was performed in R[70] v3.4.1, primarily using
472 the phytools and ape packages. Phylogenies were plotted using ggtree[71], and figures were
473 produced using ggplot2[72]. All code used in the downstream analysis is available in
474 Supplementary File 3.

475

476 Acknowledgements

477 The authors thank the sequencing team at Wellcome Sanger Institute; S Harris for access to
478 local scripts; A Wailan for discussions around rPinecone; D Domman for helpful advice and
479 discussion during analysis; M Fookes for initial pilot work and bait design for SureSelect; B
480 Molini, and C Godornes at University of Washington for provision of strains; staff at
481 University College London Hospital and clinical and sexual health staff at the Mortimer
482 Market Clinic, London for UK sample provision. MM was supported by a Wellcome Trust
483 Clinical Research Fellowship (102807). Strains from the University of Washington were
484 supported by NIH grants R01 NS34235 to CMM, and R01 AI 34616 and R01 AI 42143 to SAL.
485 MAB and NRT are supported by Wellcome funding to the Sanger Institute.

486

487 ## Author Contributions

488 Conceived and designed the study: NRT, SAL, MAB, AVN, MM. Collected and collated
489 samples: SAL, CMM, MM, AVN, PF. Performed the laboratory work: MAB, SKS, LCT. Analysed
490 the data: MAB. Wrote the initial draft of the manuscript: MAB. All authors viewed and
491 contributed to the final manuscript.

492

493 ## Competing Interests

494 The authors have no competing interests to declare.

495

496 ## References

497 1. Tampa, M., Sarbu, I., Matei, C., Benea, V. & Georgescu, S. Brief History of Syphilis. *J.*
498 *Med. Life* **7,** 4–10 (2014).

499 2. Chesson, H. W., Dee, T. S. & Aral, S. O. AIDS mortality may have contributed to the
500 decline in syphilis rates in the United States in the 1990s. *Sex. Transm. Dis.* **30,** 419–424
501 (2003).

502 3. Fenton, K. A. *et al.* Infectious syphilis in high-income settings in the 21st century. *Lancet*
503 *Infect. Dis.* **8,** 244–253 (2008).

504 4. Centers for Disease Control. Syphilis - 2016 STD Surveillance Report. (2017). Available at:
505 https://www.cdc.gov/std/stats16/Syphilis.htm. (Accessed: 2nd July 2018)

506 5. Zhou, Y. *et al.* Prevalence of HIV and syphilis infection among men who have sex with
507 men in China: a meta-analysis. *BioMed Res. Int.* **2014,** 620431 (2014).

508 6. Public Health England. Sexually transmitted infections and screening for chlamydia in
509 England, 2017. (2018).

510 7. European Centre for Disease Prevention and Control. Sexually transmitted infections in
511 Europe 2013. (2015).

512 8. Mohammed, H. *et al.* Increase in Sexually Transmitted Infections among Men Who Have
513 Sex with Men, England, 2014. *Emerg. Infect. Dis.* **22,** 88–91 (2016).

514 9. Edmondson, D. G., Hu, B. & Norris, S. J. Long-Term In Vitro Culture of the Syphilis
515 Spirochete Treponema pallidum subsp. pallidum. *mBio* **9,** e01153-18 (2018).

516 10. Lafond, R. E. & Lukehart, S. A. Biological basis for syphilis. *Clin. Microbiol. Rev.* **19,** 29–49
517 (2006).

518 11. Christiansen, M. T. *et al.* Whole-genome enrichment and sequencing of Chlamydia
519 trachomatis directly from clinical samples. *BMC Infect. Dis.* **14,** 591 (2014).

520 12. Depledge, D. P. *et al.* Specific Capture and Whole-Genome Sequencing of Viruses from
521 Clinical Samples. *PLoS ONE* **6,** e27805 (2011).

522 13. Pinto, M. *et al.* Genome-scale analysis of the non-cultivable Treponema pallidum reveals
523 extensive within-patient genetic variation. *Nat. Microbiol.* **2,** 16190 (2016).

524 14. Arora, N. *et al.* Origin of modern syphilis and emergence of a pandemic Treponema
525 pallidum cluster. *Nat. Microbiol.* **2,** 16245 (2016).

15. Marks, M. *et al.* Diagnostics for yaws eradication: insights from direct next generation sequencing of cutaneous strains of Treponema pallidum. *Clin. Infect. Dis.* (2017). doi:10.1093/cid/cix892

16. Nechvátal, L. *et al.* Syphilis-causing strains belong to separate SS14-like or Nichols-like groups as defined by multilocus analysis of 19 Treponema pallidum strains. *Int. J. Med. Microbiol.* **304,** 645–653 (2014).

17. Lukehart, S. A. *et al.* Macrolide resistance in Treponema pallidum in the United States and Ireland. *N. Engl. J. Med.* **351,** 154–158 (2004).

18. Šmajs, D., Paštěková, L. & Grillová, L. Macrolide Resistance in the Syphilis Spirochete, Treponema pallidum ssp. pallidum: Can We Also Expect Macrolide-Resistant Yaws Strains? *Am. J. Trop. Med. Hyg.* **93,** 678–683 (2015).

19. WHO. Eradication of yaws – the Morges Strategy. *Wkly Epidemiol Rec* **87,** 189–194 (2012).

20. Mitjà, O. *et al.* Re-emergence of yaws after single mass azithromycin treatment followed by targeted treatment: a longitudinal study. *The Lancet* **391,** 1599–1607 (2018).

21. Giacani, L. *et al.* Complete Genome Sequence and Annotation of the Treponema pallidum subsp. pallidum Chicago Strain. *J. Bacteriol.* **192,** 2645–2646 (2010).

22. Giacani, L. *et al.* Complete Genome Sequence of the Treponema pallidum subsp. pallidum Sea81-4 Strain. *Genome Announc.* **2,** (2014).

23. Sun, J. *et al.* Tracing the origin of Treponema pallidum in China using next-generation sequencing. *Oncotarget* **7,** 42904–42918 (2016).

547 24. Matějková, P. *et al.* Complete genome sequence of Treponema pallidum ssp. pallidum
548 strain SS14 determined with oligonucleotide arrays. *BMC Microbiol.* **8,** 76 (2008).

549 25. Pětrošová, H. *et al.* Resequencing of Treponema pallidum ssp. pallidum Strains Nichols
550 and SS14: Correction of Sequencing Errors Resulted in Increased Separation of Syphilis
551 Treponeme Subclusters. *PLOS ONE* **8,** e74319 (2013).

552 26. Tong, M.-L. *et al.* Whole genome sequence of the Treponema pallidum subsp. pallidum
553 strain Amoy: An Asian isolate highly similar to SS14. *PLoS ONE* **12,** (2017).

554 27. Čejková, D. *et al.* Whole Genome Sequences of Three Treponema pallidum ssp.
555 pertenue Strains: Yaws and Syphilis Treponemes Differ in Less than 0.2% of the Genome
556 Sequence. *PLoS Negl. Trop. Dis.* **6,** e1471 (2012).

557 28. Pětrošová, H. *et al.* Whole Genome Sequence of Treponema pallidum ssp. pallidum,
558 Strain Mexico A, Suggests Recombination between Yaws and Syphilis Strains. *PLoS Negl.*
559 *Trop. Dis.* **6,** e1832 (2012).

560 29. Suchard, M. A. *et al.* Bayesian phylogenetic and phylodynamic data integration using
561 BEAST 1.10. *Virus Evol.* **4,** (2018).

562 30. Wailan, A. M. *et al.* rPinecone: Define sub-lineages of a clonal expansion via a
563 phylogenetic tree. *bioRxiv* 404624 (2018). doi:10.1101/404624

564 31. Stamm, L. V. & Bergen, H. L. A Point Mutation Associated with Bacterial Macrolide
565 Resistance Is Present in Both 23S rRNA Genes of an Erythromycin-Resistant Treponema
566 pallidum Clinical Isolate. *Antimicrob. Agents Chemother.* **44,** 806–807 (2000).

567 32. Matějková, P. *et al.* Macrolide treatment failure in a case of secondary syphilis: a novel
568 A2059G mutation in the 23S rRNA gene of Treponema pallidum subsp. pallidum. *J. Med.*
569 *Microbiol.* **58,** 832–836 (2009).

570 33. Molini, B. J. *et al.* Macrolide Resistance in Treponema pallidum Correlates With 23S
571 rDNA Mutations in Recently Isolated Clinical Strains. *Sex. Transm. Dis.* **43,** 579–583
572 (2016).

573 34. Hunt, M. *et al.* ARIBA: rapid antimicrobial resistance genotyping directly from
574 sequencing reads. *Microb. Genomics* **3,** (2017).

575 35. Weill, F.-X. *et al.* Genomic history of the seventh pandemic of cholera in Africa. *Science*
576 **358,** 785–789 (2017).

577 36. Hadfield, J. *et al.* Comprehensive global genome dynamics of Chlamydia trachomatis
578 show ancient diversification followed by contemporary mixing and recent lineage
579 expansion. *Genome Res.* **27,** 1220–1229 (2017).

580 37. Strouhal, M. *et al.* Complete genome sequences of two strains of Treponema pallidum
581 subsp. pertenue from Ghana, Africa: Identical genome sequences in samples isolated
582 more than 7 years apart. *PLoS Negl. Trop. Dis.* **11,** e0005894 (2017).

583 38. Grimes, M. *et al.* Two Mutations associated with Macrolide Resistance in Treponema
584 pallidum: Increasing Prevalence and Correlation with Molecular Strain Type in Seattle,
585 Washington. *Sex. Transm. Dis.* **39,** 954–958 (2012).

586 39. WHO. WHO guidelines for the treatment of *Treponema pallidum* (syphilis). (2016).

587 40. Centers for Disease Control. Sexually Transmitted Diseases Treatment Guidelines, 2015.
588 *Morb. Mortal. Wkly. Rep.* **64,** (2015).

589 41. Marra, C. M. *et al.* Antibiotic Selection May Contribute to Increases in Macrolide-
590 Resistant Treponema pallidum. *J. Infect. Dis.* **194,** 1771–1773 (2006).

591 42. Hicks, L. A., Taylor, T. H. & Hunkler, R. J. U.S. Outpatient Antibiotic Prescribing, 2010. *N.*
592 *Engl. J. Med.* **368,** 1461–1462 (2013).

593 43. Kong, F. Y. S. *et al.* Pharmacokinetics of a single 1g dose of azithromycin in rectal tissue
594 in men. *PLOS ONE* **12,** e0174372 (2017).

595 44. Nurse-Findlay, S. *et al.* Shortages of benzathine penicillin for prevention of mother-to-
596 child transmission of syphilis: An evaluation from multi-country surveys and stakeholder
597 interviews. *PLOS Med.* **14,** e1002473 (2017).

598 45. Chen, X.-S. *et al.* High prevalence of azithromycin resistance to Treponema pallidum in
599 geographically different areas in China. *Clin. Microbiol. Infect.* **19,** 975–979 (2013).

600 46. Lu, H. *et al.* High frequency of the 23S rRNA A2058G mutation of *Treponema pallidum* in
601 Shanghai is associated with a current strategy for the treatment of syphilis. *Emerg.*
602 *Microbes Infect.* **4,** e10 (2015).

603 47. Taylor, M. *et al.* Revisiting strategies to eliminate mother-to-child transmission of
604 syphilis. *Lancet Glob. Health* **6,** e26–e28 (2018).

605 48. Baker, S., Thomson, N., Weill, F.-X. & Holt, K. E. Genomic insights into the emergence
606 and spread of antimicrobial-resistant bacterial pathogens. *Science* **360,** 733–738 (2018).

607 49. WHO. Global action plan on antimicrobial resistance. (2015).

608 50. Lukehart, S. A. & Marra, C. M. Isolation and laboratory maintenance of Treponema
609 pallidum. *Curr. Protoc. Microbiol.* **Chapter 12,** Unit 12A.1 (2007).

610 51. Wood, D. E. & Salzberg, S. L. Kraken: ultrafast metagenomic sequence classification
611 using exact alignments. *Genome Biol.* **15,** R46 (2014).

612 52. Bolger, A. M., Lohse, M. & Usadel, B. Trimmomatic: a flexible trimmer for Illumina
613 sequence data. *Bioinformatics* **30,** 2114–2120 (2014).

614 53. Quinlan, A. R. & Hall, I. M. BEDTools: a flexible suite of utilities for comparing genomic
615 features. *Bioinformatics* **26,** 841–842 (2010).

616 54. Li, H. Aligning sequence reads, clone sequences and assembly contigs with BWA-MEM.
617 *arXiv* (2013). doi:1303.3997v1 [q-bio.GN]

618 55. Van der Auwera, G. A. *et al.* From FastQ data to high confidence variant calls: the
619 Genome Analysis Toolkit best practices pipeline. *Curr. Protoc. Bioinforma. Ed. Board*
620 *Andreas Baxevanis Al* **11,** 11.10.1-11.10.33 (2013).

621 56. Li, H. *et al.* The Sequence Alignment/Map format and SAMtools. *Bioinformatics* **25,**
622 2078–2079 (2009).

623 57. Croucher, N. J. *et al.* Rapid phylogenetic analysis of large samples of recombinant
624 bacterial whole genome sequences using Gubbins. *Nucleic Acids Res.* gku1196 (2014).
625 doi:10.1093/nar/gku1196

626 58. Nguyen, L.-T., Schmidt, H. A., von Haeseler, A. & Minh, B. Q. IQ-TREE: A Fast and
627 Effective Stochastic Algorithm for Estimating Maximum-Likelihood Phylogenies. *Mol.*
628 *Biol. Evol.* **32,** 268–274 (2015).

629 59. Lewis, P. O. A Likelihood Approach to Estimating Phylogeny from Discrete Morphological
630 Character Data. *Syst. Biol.* **50,** 913–925 (2001).

631 60. Kalyaanamoorthy, S., Minh, B. Q., Wong, T. K. F., Haeseler, A. von & Jermiin, L. S.
632 ModelFinder: fast model selection for accurate phylogenetic estimates. *Nat. Methods*
633 **14,** 587–589 (2017).

634 61. Kimura, M. Estimation of evolutionary distances between homologous nucleotide
635 sequences. *Proc. Natl. Acad. Sci.* **78,** 454–458 (1981).

636 62. Soubrier, J. *et al.* The Influence of Rate Heterogeneity among Sites on the Time
637 Dependence of Molecular Rates. *Mol. Biol. Evol.* **29,** 3345–3358 (2012).

638 63. Hoang, D. T., Chernomor, O., Haeseler, A. von, Minh, B. Q. & Le, V. S. UFBoot2:
639 Improving the Ultrafast Bootstrap Approximation. *bioRxiv* 153916 (2017).
640 doi:10.1101/153916

641 64. Minh, B. Q., Nguyen, M. A. T. & von Haeseler, A. Ultrafast Approximation for
642 Phylogenetic Bootstrap. *Mol. Biol. Evol.* **30,** 1188–1195 (2013).

643 65. Pupko, T., Pe, I., Shamir, R. & Graur, D. A Fast Algorithm for Joint Reconstruction of
644 Ancestral Amino Acid Sequences. *Mol. Biol. Evol.* **17,** 890–896 (2000).

645 66. Rambaut, A., Lam, T. T., Max Carvalho, L. & Pybus, O. G. Exploring the temporal
646 structure of heterochronous sequences using TempEst (formerly Path-O-Gen). *Virus*
647 *Evol.* **2,** (2016).

648 67. Baele, G. & Lemey, P. Bayesian evolutionary model testing in the phylogenomics era:
649 matching model complexity with computational efficiency. *Bioinformatics* **29,** 1970–
650 1979 (2013).

651 68. Baele, G. *et al.* Improving the accuracy of demographic and molecular clock model
652 comparison while accommodating phylogenetic uncertainty. *Mol. Biol. Evol.* **29,** 2157–
653 2167 (2012).

654 69. Rieux, A. & Khatchikian, C. E. tipdatingbeast: an r package to assist the implementation
655 of phylogenetic tip-dating tests using beast. *Mol. Ecol. Resour.* **17,** 608–613

656 70. R Core Team. *R: A Language and Environment for Statistical Computing.* (R Foundation
657 for Statistical Computing, 2014).

658 71. Yu, G., Smith, D., Zhu, H., Guan, Y. & Lam, T. T.-Y. *ggtree: an R package for visualization*
659 *and annotation of phylogenetic tree with different types of meta-data*.

660 72. Wickham, H. *ggplot2: Elegant Graphics for Data Analysis*. (Springer-Verlag, 2009).

661

662 ## Supplementary Figures

663 Supplementary Figure 1. Root-to-tip regression analysis of tip dates against branch lengths
664 showing a correlation of 0.443 and R2 of 0.196, providing evidence for temporal signal in
665 the Maximum Likelihood tree, performed in TempEst using clinically derived genomes from
666 both Nichols and SS14 lineages. Plots show tip points and linear regression (with standard
667 error) for full timeline (A) and zoomed in to only include sampled tipdates (B). Each data
668 point is coloured grey, with darker shading indicating multiple overlapping points.

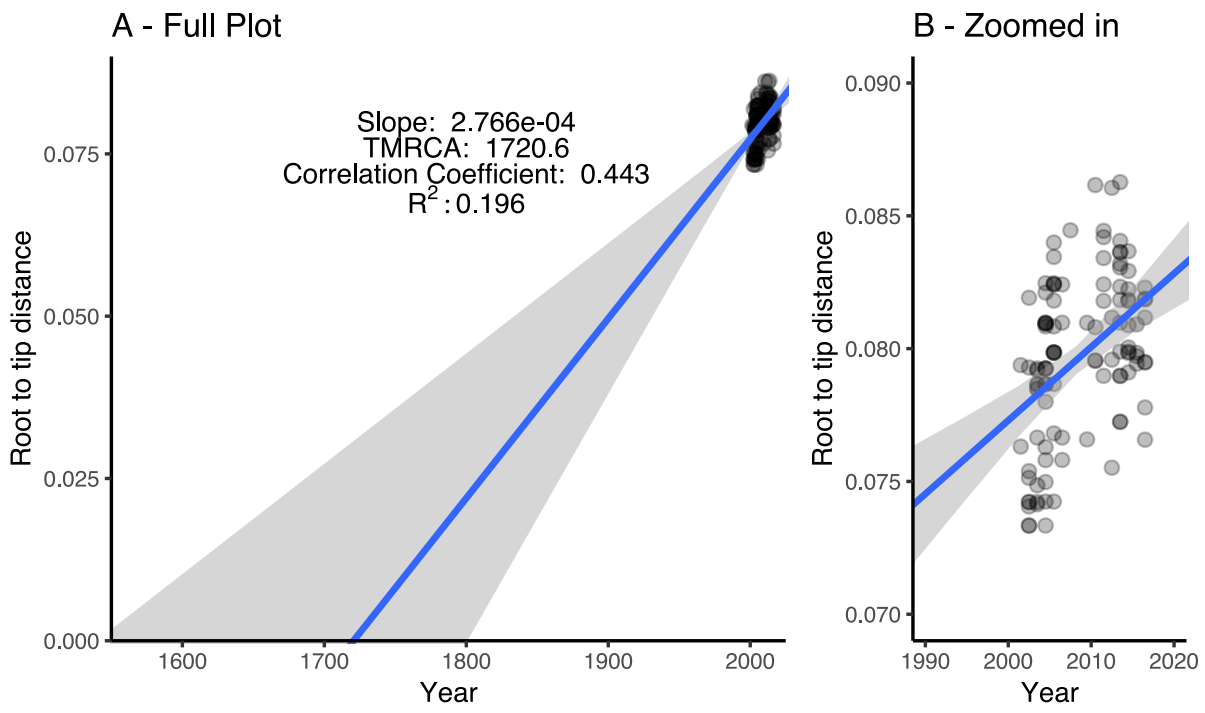

669

670

671

672 Supplementary Figure 2. Tip date resampling analysis performed using twenty datasets with
673 randomised tip dates generated from the original Strict Clock analysis and run in BEAST
674 under the same conditions. Median clock rate for the real tree was 2.26 x 10^{-7}, whilst all

675 randomly assigned datasets gave substantially lower clock rates, with the highest median
676 clock rate obtained at 1.90 x 10^{-12}. This indicates that the temporal signal observed in our
677 tree was not obtained by chance, and provides further evidence for a temporal signal in the
678 multiple sequence alignment.

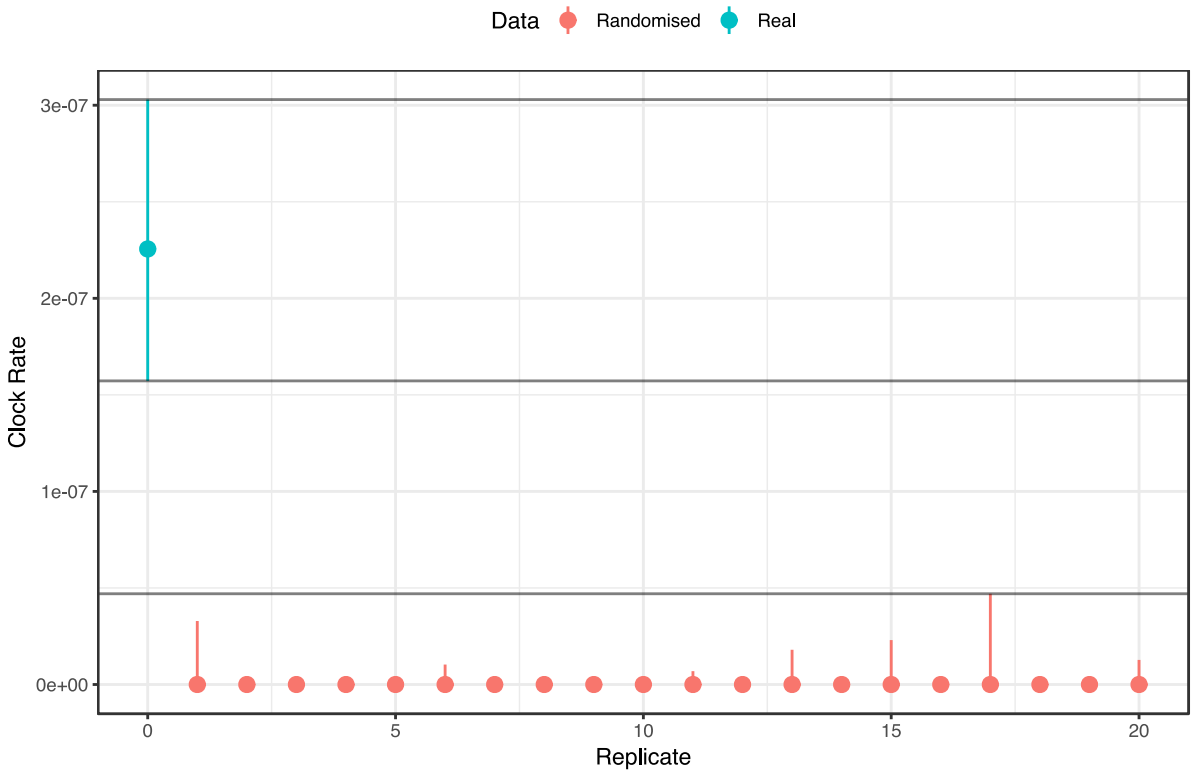

679

680

681

682 Supplementary Table 1. Full sample metadata (Excel Sheet) for this study, including
683 sequence naming used in this paper, in other publications, and on GenBank, ENA Accessions
684 for all new genomes, as well as results of lineage and sub-lineage typing and inference of
685 genotypic macrolide resistance.

686

687 Supplementary Table 2. List of genomic regions behaving in a non-clocklike manner and

688 masked due to hypervariable, recombining or repetitive elements.

689

690 Supplementary File 3. Rnotebook (HTML format) containing all downstream code used to

691 generate primary figures and statistics.